Chapter 7: Linking PET Imaging in Humans to the Grasping Model

---

In this chapter, we relate the model of grasp generation, derived in large part from monkey neurophysiological data, to the human functional anatomy involved in grasping. First, a technique referred to as *synthetic PET imaging* is applied to the model, from which we derive a set of predictions for what we expect to observe in a human experiment. We then describe a human PET experiment that looks at the processing of instruction stimuli in a conditional task, as well as at the relative representation of different grasp programs. Finally, through comparison of the synthetic PET predictions and human experimental results, we reflect on how the model may be further refined.

Synthetic PET Imaging

$H_2{}^{15}O$ positron emission tomography (PET) is an imaging technique that allows the measurement of regional cerebral blood flow (rCBF). Because rCBF appears to be related to the local synaptic activity within a region (Brownell, Budinger, Lauterbur, & McGeer, 1982), it is possible to observe differences in the measured rCBF as a function of the task that a subject performs. As a result, the technique has significantly contributed to our recent understanding the functional anatomy of the human brain (e.g., (Barbur, Watson, Frackowiak, & Zeki, 1993; Decety, et al., 1994; Grafton, et al., 1995; Silverman, Grossman, Galetta, Liu, Rosenquist, & Alavi, 1995)).

Current resolution of the technique is on the order of 1.5mm in each spatial dimension, and temporally is about 80 seconds. This level of information differs considerably from what is available in neurophysiological experiments in monkey, where we are able to examine individual cells and resolve single spikes, but have tremendous difficulties in examining entire circuits. It is thus desirable to develop techniques that allow us to draw conclusions in one domain from experimental results in the other.

Synthetic PET imaging (Arbib, Bischoff, Fagg, & Grafton, 1995) has been proposed as one such mechanism for relating these different levels of experimentation through the construction of a computational model. The low-level details of the model described in this thesis have been derived primarily from a combination of neurophysiological (monkey) results and computational constraints. From the model, we extract a measure of regional synaptic activity, which can then be compared to rCBF results in human PET experiments.

Computation of the Synthetic PET Measure

The synaptic activity of a region A under condition X is computed from the model as follows:

$$SA_A^X = \int_t \sum_{j \in A} \sum_i a_i(t) \left| w_{ij} \right| dt \qquad (7.1)$$

where:

$a_j(t)\left|w_{ij}\right|$ is the activity of the synapse connecting unit j to unit i at time t.

i iterates over all presynaptic units to unit j (which may or may not be members of region A; see Figure 7.1).

j iterates over all neurons in region A.

The measure of instantaneous synaptic activity in region A is then integrated over the time required to perform a task (which might involve multiple trials).

The simulated synaptic activity of a region can then be compared over several conditions. Here we define the *relative synaptic activity* for region A under conditions X and Y as:

$$rSA_A^q = \frac{SA_A^q}{\underset{z \in \{X,Y\}}{Max}\left\{SA_A^z\right\}} \tag{7.2}$$

where:

$$q \in \{X, Y\}$$

And the *change in relative synaptic activity* from Y to X is:

$$\Delta rSA_A^{Y \to X} = rSA_A^X - rSA_A^Y \tag{7.3}$$

Note that the positive and negative projections into a region are treated equally in their contribution to the synthetic PET measure (due to the absolute value operator applied to the connection weight in equation 7.1). Thus, from the PET measure alone, it is impossible to distinguish the case in which a positive input is given from the situation where an equally negative input is given.

Synthetic PET Imaging for the Grasping Model

Note that in the model, each column receives three distinct types of projections (priming, support, and trigger). In computation of the synthetic PET measures, the contributions of these different inputs are assumed to be weighted equally, and are simply summed in computing the column's contribution to the region's rCBF measure.

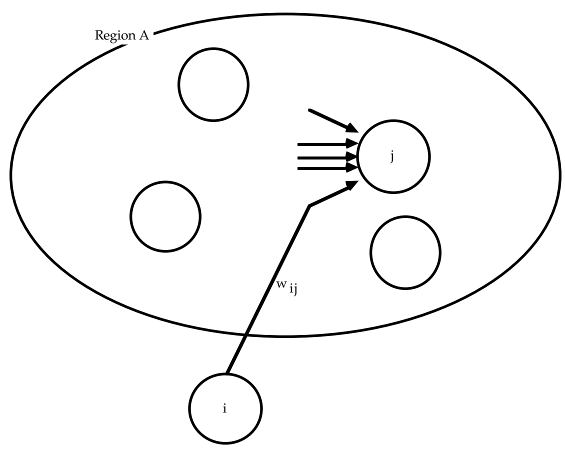

Figure 7.1: Neural elements involved in computing the synaptic activity for a simulated brain region.

In what follows, we present the results of two different synthetic PET experiments, which serve as predictions for what we expect when the experiments are performed in the human.

Conditional Task

When a delayed instruction stimulus is used to inform a subject how to grasp an object, what brain regions are involved above and beyond the case where the subject knows a priori which of the two grasps to perform? In chapter 6 (prediction #3), we analyzed how the model performs in such a situation, and examined the single cell and population-level behaviors of several key regions. Here, we present the synthetic PET measures taken during execution of a precision grasp under the conditional and non-conditional tasks.

Figure 7.3 A plots the relative synaptic activity measures for the two tasks. Only regions in the model that demonstrate a change in synaptic activity from one task to the other are shown. The most significant change predicted by the model is the level of activity exhibited by area F2 (dorsal premotor cortex). Its high level of activity in the conditional task is due to the fact that this region is only involved when the model must map an arbitrary stimulus to a motor program (in this case, a grasp). In the non-conditional task, the region does not receive IS inputs, and thus its synaptic activity is dominated by the general background activity in the region.

The additional IS inputs in the conditional task have a second-order effect on the network, as reflected in the small changes in activity in F5, BG, and AIP (Figure 7.2). The increased synaptic activity in F5 is due to the additional inputs from F2 (into the supporting inputs of some columns in F5). These inputs also cause an increase in the region's *activity level*, which is passed on through excitatory connections to both AIP and BG (the latter appears in the figure as the recurrent inhibitory connections back to F5 and AIP).

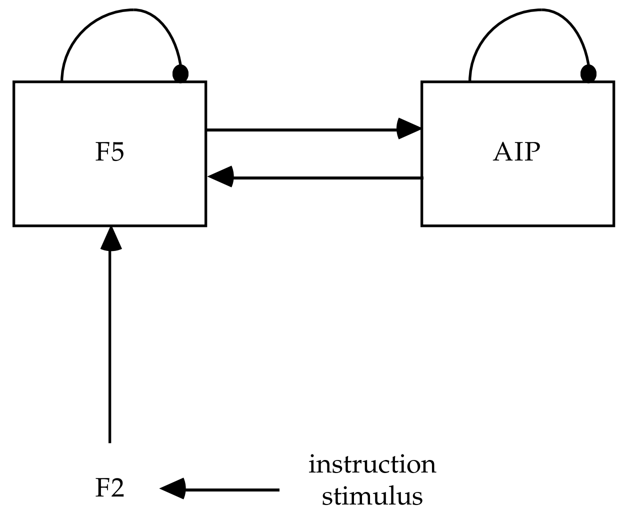

Figure 7.2: Functional interactions of F2, F5, and AIP.

An important ability of the synthetic PET technique is that the positive and negative contributions to the synthetic PET measure can be differentiated. Figures 7.4A,B demonstrate the positive and negative contributions to the overall PET measure in the conditional/non-conditional task comparison. Note that although the positive contributions to the F5 and AIP essentially dominate the full PET measure, we also see small increases in the negative inputs into these regions. These inhibitory signals are due to the recurrent inputs through the BG. This is additional evidence that both F5 and AIP are experiencing increases in their overall activity (not just of synaptic activity).

Precision versus Side Opposition

One observation made by (Rizzolatti, et al., 1988) was that in F5, the number of neurons involved in the execution of the precision pinch was greater than those involved in either the side opposition or the power grasp (the fewest neurons were observed in the latter case). In the construction of the model, this information was used to select the distribution of neurons for each type of grasp. An important question is how this distribution is reflected in the PET measures. Here, we compare these measures for the precision pinch and side opposition (the protocol is the same as in prediction #3, although we compare the two non-conditional tasks).

Figure 7.3B illustrates a general increase in synaptic activity in many of the model's regions for the precision pinch case. Although there is an increase in the number of active units only in F5 and AIP (from one condition to the other), we observe a subsequent increase in synaptic

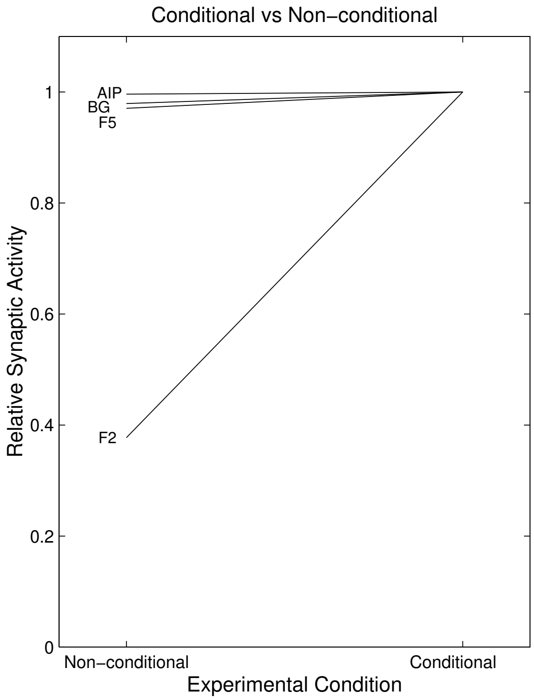

(A)

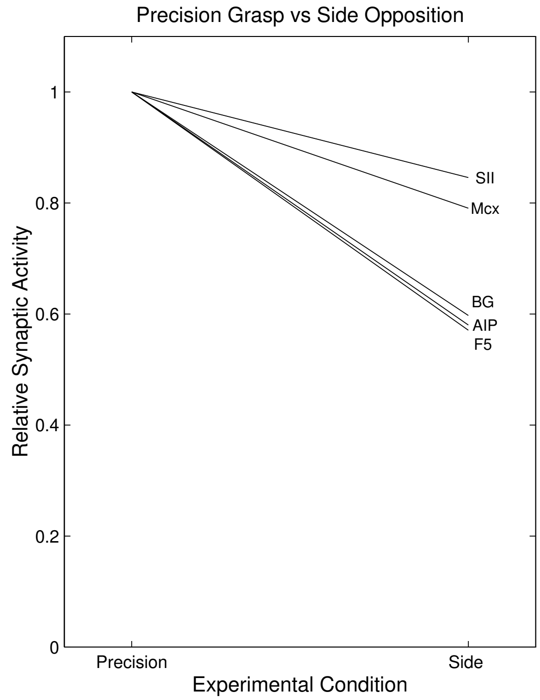

(B)

Figure 7.3: Predictions of relative synaptic activity changes for (A) a non-conditional task and a conditional task, and (B) a precision pinch and a side opposition.

activity in BG, Mcx, and SII. The increase in synaptic activity in BG actually reflects a true increase in the region's activity level, as indicated by the increase in inhibitory inputs back into AIP and F5 (Figure 7.4D).

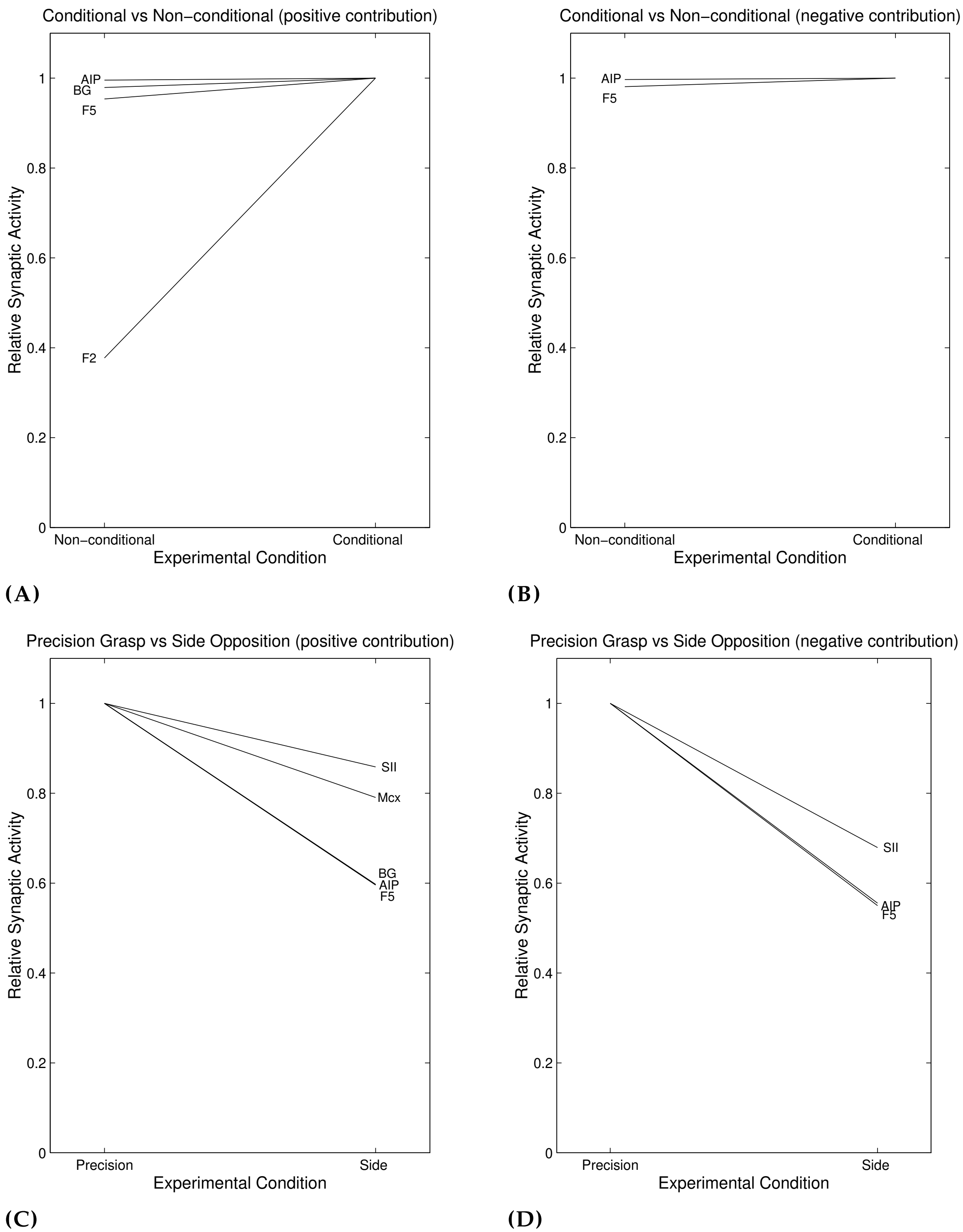

Figure 7.4: Positive and negative synapse contributions to the synaptic activity measure for the conditional/non-conditional task (A and B), and for the precision pinch/side opposition task (C and D).

Human Grasping Experiment

The synthetic PET experiments that have been presented have asked some important questions about how instruction stimuli are mapped to arbitrary motor programs, and about the relative representation of different grasps. In this section, we present a human PET experiment in which both of these questions are addressed.

Materials and Methods

Subjects

Six normal, right-handed subjects participated in the study.

Tasks

Subjects were asked to repeatedly perform grasping movements over the 90 second scanning period. The targets of grasping were mounted on the experimental apparatus shown in Figure 7.5. Each of three stations mounted on the apparatus consisted of both a rectangular block that could be grasped using a power grasp, and a pair of plates (mounted in a groove on the side of the block; see inset of Figure), which could be grasped using a precision pinch (thumb and index finger). A force sensitive resistor (FSR) material, mounted on the front and back of the block, detected when a solid power grasp had been established. The two plates were attached to a pair of mechanical micro-switches, which detected when a successful precision pinch had been executed. A bi-colored LED at each station was used to instruct the subject as to the next target of movement. A successful grasp of this next target was indicated to the subject by a change in the color of the LED. The subject then held the grasp position until the next target was given. Targets were presented every 3 +/- 0.1 seconds.

In the first grasping condition, subjects repeatedly performed a power grasp to the indicated block. The target block was identified by the turning on of the associated LED (green in color). When the subject grasped the block, the color of the LED changed from green to red. For the second condition a precision pinch was used; the target was identified in the same manner as the first condition. In the third grasping condition (conditional task), the initial color of the LED instructed the subject to use either a precision pinch (green) or a power grasp (red). When contact was established, the LED changed to the opposite color.

In the fourth (control) condition, the subjects were instructed to simply fixate on the currently lit LED and not make movements of the arm or hand. The lit LED changed from one position to another at the same rate and variability as in the grasping task.

Each of the four conditions were performed by each subject three times. The order of condition presentation was selected at random. In addition, the order of trial presentation was randomly selected, as was the LED color in the conditional task.

Prior to scanning, subjects practiced each of the grasping conditions for several minutes.

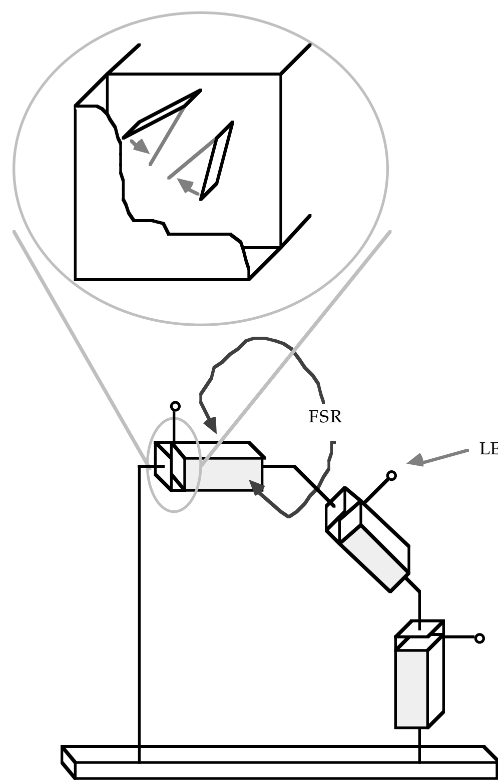

Figure 7.5: Apparatus used in PET experiment. Each of three stations can be grasped in two ways: precision pinch of the two plates in the grove (inset), or power grasp of the block.

Performance Measures

Reaction time data was collected by the control computer as the subjects performed the task. The computer logged time required to release the current object in response to a new target, the time required to establish a grasp on the new object, and whether the established grasp was correct. In addition, the subject's hand position was tracked using a Polhemus tracking device (Polhemus, Colchester, VT), which measures six DOF of wrist position. A VPL DataGlove (VPL Research, Inc) measured the joint angle of the two proximal joints of each finger. Both types of data were sampled at 30 Hz.

Imaging

rCBF images were collected using a Siemens 953/A tomograph. Subjects were injected intravenously with $H_2{}^{15}O$ at the start of scanning and performance of the behavioral task.

Image Analysis

Prior to statistical analysis, the rCBF images were aligned to a reference MRI atlas that was defined relative to the Talairach coordinate system (Talairach & Tournoux, 1988). This alignment was accomplished by first performing a within-subject alignment of the subject's 12 scans using an automated registration algorithm (Woods, Cherry, & Maxxiotta, 1992). Next, a mean PET image for each subject was computed. The mean PET image was then coregistered with the standardized MRI atlas (Woods, Mazziotta, & Cherry, 1993). Finally, the individual rCBF images were resliced (combining the within-subject and mean PET image-to-atlas transformations) into the coordinate frame of the standardized MRI atlas.

The rCBF images were then smoothed. A common volume mask was computed, which marks the voxels for which data is available in all scans (from all subjects). The smoothed images were then normalized to each other.

Statistical Tests

Task-related effects in rCBF were extracted using a 2-way analysis of variance (ANOVA) applied to the image set. The sources of variance in the model were *task* and *subject* (repetitions were assumed to not be a source of variance).

An F-map of task effects was finally computed for each voxel, the results of which are thresholded and overlayed with the MRI atlas.

Results

Behavioral Results

For each trial during the scanning, subject reaction time to target presentation (turning on of the LEDs) were measured. Both the time required to release the currently held object and the time required to grasp the next were recorded. Figure 7.6A demonstrates that there was relatively little effect on reaction time as a function of task, although the conditional task required on average about 119ms longer than the non-conditional tasks (well within 1 standard deviation). Hence, the amount of time involved in transport of the hand and establishment of the grasp is essentially constant across the tasks. In addition, little effect was observed when precision grasp trials were compared to power grasp trials in the conditional task (B).

Finally, little change was seen in performance as a function of task repetition (C, D, and E). This indicates that little or no learning occurred during the course of the scans, and we can discount any repetition effects in our analysis.

Imaging Studies

The set of regions more significantly active ($p < 0.005$) in the conditional task as compared to the movement conditions (combination of precision and power tasks) are shown in Figure 7.8 [1]; the most significant ($p < 0.001$) regions are summarized in Table 7.1.

The most highly active region in this comparison is the contralateral dorsal premotor cortex. In monkey, this region is thought to be involved in the arbitrary association of stimuli with the preparation of motor programs (Evarts, et al., 1984; Kurata & Hoffman, 1994; Kurata & Wise, 1988; Mitz, et al., 1991; Wise & Mauritz, 1985), although this region has been traditionally thought of as a limb-related area, and not one involving distal movements. The ipsilateral dorsal premotor cortex is also active, although the degree of activity is

---

[1] The color plates corresponding to Figures 7.11 and 7.10 may be found at http://www.usc.edu/dept/robotics/personal/af0a/thesis/

significantly less, and the centroid of activity is more mesial and frontal from the contralateral side.

A site in the contralateral inferior parietal cortex is also significantly active. This region is located near the anterior bank of the intra-parietal sulcus, and may be related to the monkey AIP. In addition, several visual processing sites are reasonably active: two distinct locations in the ipsilateral area 18, and one area in the superior occipital lobe (near the area 18/19 boundary). Finally, a site within the cerebellar cortex shows moderate activation.

The areas more significantly active ($p < 0.01$) in the precision grasp condition as compared with the power grasp condition are shown in Figure 7.9; the most significant ($p < 0.005$) sites are summarized in Table 7.2. The most significant sites of activation are in the contralateral superior occipital lobe (identical site as in the above comparison), and the contralateral supplementary motor area (SMA-proper; near the boundary with area 4).

Less active, but still above threshold, include the ipsilateral dorsal premotor cortex (different site than in the conditional comparison), the contralateral cerebellar vermis, contralateral inferior parietal cortex, contralateral area 18, and contralateral area 7. As in the conditional comparison, the inferior parietal cortex site is located near the anterior bank of the intra-parietal sulcus. However, this site is more lateral and slightly more frontal.

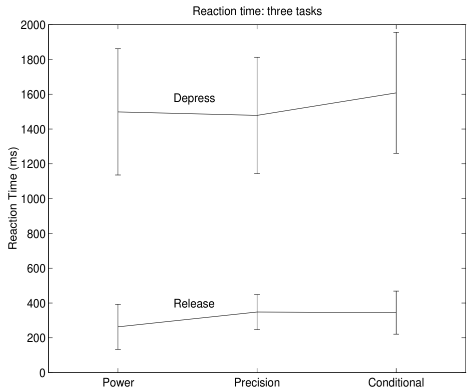

(A)

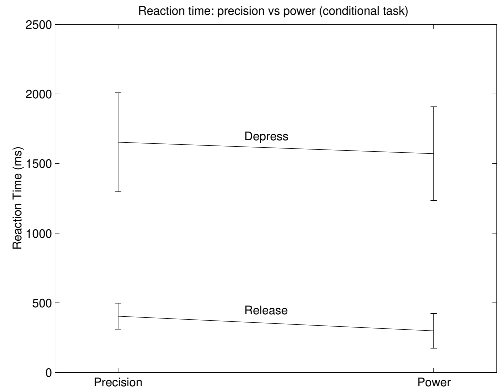

(B)

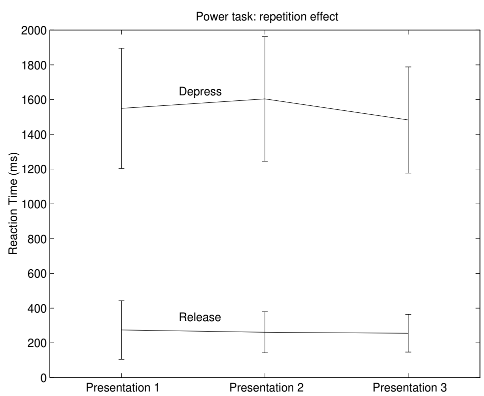

(C)

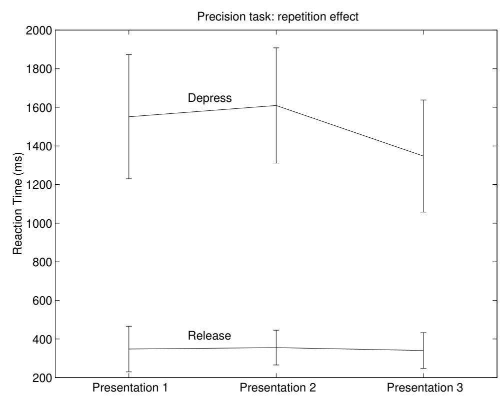

(D)

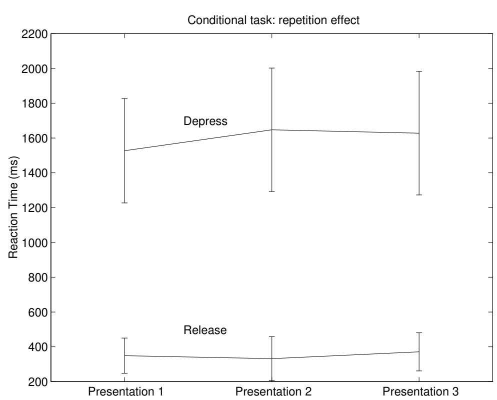

(E)

Figure 7.6: Reaction times for both the release of the switch and the depression of the next switch: (A) comparison between the three movement tasks; (B) comparison of precision and power trials within the conditional task; and repetition effects for power grasp (C), precision pinch (D), and the conditional task (E). The error bars indicate 1 STD.

Anatomic Location	Talairach Coordinates (mm)			Volume (mm^3)
	X	Y	Z	
L Dorsal Premotor Cortex (postcentral gyrus)	-25.35	-10.52	51.34	1340
L Inferior Parietal Cortex (supramarginal gyrus; anterior bank of the intra-parietal sulcus)	-32.98	-56.86	33.00	520
R Area 18 (occipital lobe, lingual gyrus)	7.66	-98.67	-6.44	476
L Area 18/19 (superior occipital lobe)	-24.91	-72.72	25.34	192
R Area 18 (occipital lobe, lingual gyrus)	8.37	-69.81	-11.68	74
R Cerebellar Cortex*	7.5	-66.0	-22.5	433
R Dorsal Premotor Cortex (frontal medial gyrus)*	15.21	-2.27	49.81	165

Table 7.1: Significant regions of activity ($p < 0.001$): conditional - non-conditional (combined precision and power). * = only significant ($p < 0.001$) in 5 subjects (certain regions were missed on the scanner with one subject).

Anatomic Location	Talairach Coordinates (mm)			Volume (mm^3)
	X	Y	Z	
L Area 18/19 (superior occipital lobe)	-26.74	-74.39	25.74	176
L (somewhat bilateral) SMA Proper (frontal medial gyrus)	-6.74	-37.22	66.56	493
R Dorsal Premotor Cortex (frontal medial gyrus)	18.28	-12.01	65.10	179
L Cerebellar Vermis*	-4.69	-60.09	-20.12	57
L Inferior Parietal Cortex (supramarginal gyrus; anterior bank of the intra-parietal sulcus)*	-50.21	-47.27	37.34	196
L Area 18 (occipital lobe, lingual gyrus)*	-11.24	-80.84	0.11	216
L Area 7 (superior parietal lobe)*	-28.52	-56.87	54.76	209

Table 7.2: Significant regions of activity ($p < 0.005$) : precision pinch - power grasp. * = only significant ($p < 0.005$) in 5 subjects (certain regions were missed on the scanner with one subject).

Comparison of PET and synthetic PET Results

Precision versus Side Opposition/Power Grasp

In the comparison of precision pinch and side opposition, the model predicts an increase of synaptic activity in both F5 and AIP in the precision pinch case. Although we see an increase in activity in the inferior parietal area in the human experiment, we fail to see any such change in the ventral premotor cortex (specifically F5). Two explanations are possible for this negative result. First, it is possible that for stereotypical grasps, that F5 does not play a significant role. Rather, it is the cerebellum that is that is responsible for the execution of the grasp.

The second possibility assumes that F5 is involved in the grasp, but the effect is masked by force-related activity in the region. In the human experiment, performance of the power grasp required a reasonable level of force to be applied to the block before the LED would indicate to the subject that a grasp had been detected. In monkey, force-related activity has been observed in F5 (Heppreymond, Husler, Maier, & Qi, 1994). The implication is that even though there are fewer neurons involved in encoding the power grasp, they are achieving a higher level of activity because of the force requirements of the task. Thus, the rCBF measures could still be relatively similar in both conditions.

Conditional vs Non-Conditional Task

The model predicts that in the conditional task, we would expect to see a much higher level of activation in F2 (dorsal premotor cortex), some activation of F5, and a slight activation of AIP. The human experiment confirmed the F2 result, but failed to do so in F5 and AIP. In fact, the results were essentially opposite: in human, we see an activation of the inferior parietal cortex (AIP), but no significant activation of ventral premotor cortex.

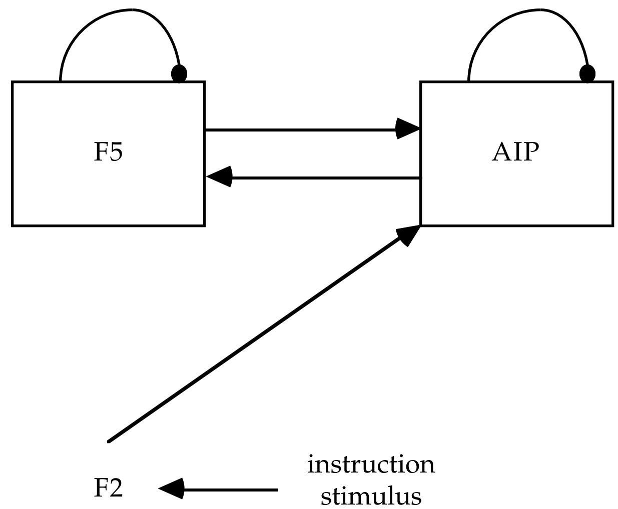

Figure 7.7: Updated functional model. The information from F2 flows into the circuit through a projection into AIP.

Consider the functional connectivity of these regions in the model (Figure 7.2). In practice, the strength of projection from F2 to F5 is essentially a free parameter. In other words, there is a wide range of values over which the model will correctly perform the conditional and non-conditional tasks. The implication is that by tuning this parameter, we can control this projection's contribution to the synaptic activity measure in F5. However, it is always the case that the difference in AIP synaptic activity from the non-conditional to the conditional task will be less than the difference observed in F5. Why is this the case? By increasing the projection strength from F2 to F5, we observe both an increase in F5 activity and synaptic activity. The increase in F5 activity, however, is attenuated by the recurrent inhibitory projection through the BG. Thus the signal that is then passed on to AIP from F5 does not reflect the full magnitude of the signal received from F2.

The conclusion is that although we can adjust the free parameter to match one or the other observations in the human experiment (of either F5 or AIP changes), the model cannot reflect both at the same time. One possibility for repairing this problem in the model is to reroute the F2 information so that it enters the grasp decision circuitry through AIP, rather than F5 (Figure 7.7). As a result, we will see an increase in activity in AIP due to F2 activation, and only an attenuated signal will be passed on to F5 (and thus, only a small increase in synaptic activity will be observed).

Summary

Neurological experiments performed in monkey and human fundamentally yield different types of information about the computational structure and function of the brain. In human, PET and fMRI techniques allow us to achieve a global view of the systems involved in performing a task, but at the expense of a very coarse spatial and temporal resolution. In monkey, on the other hand, recording of single unit (or small populations of units) presents significant challenges as we attempt to understand what a region is computing, let alone an entire circuit of regions. It is thus important to develop techniques that allow experimental results at both levels to be brought together as we attempt to understand the different systems.

In this chapter, we have explored the use of a technique referred to as synthetic PET imaging for just this purpose. The low-level details of the grasping model presented in earlier chapters has been derived primarily from neurophysiological results obtained in monkey. Using the synthetic PET approach, we extract from the model measures of regional synaptic activity as the model performs a variety of tasks. These measures of synaptic activity are then compared to rCBF (regional cerebral blood flow) observed during human PET experiments as the subjects perform tasks similar to those performed by the model. In some cases, the human results provide confirmation of the model behavior. In other cases, where there is a mismatch between model prediction and human results, it is possible (as we have shown) to use these negative results to further refine and constrain the model.